NAVAL POSTGRADUATE SCHOOL
MONTEREY, CALIFORNIA

THESIS

SOOT PARTICLE DENSITY DETERMINATION FROM A LASER EXTINCTION MULTIPASS TECHNIQUE

by

Gregory E. Glaros

September, 1994

Thesis Advisor: Oscar Biblar
Co-Advisor: David W. Netzer

Approved for public release; distribution is unlimited.

REPORT DOCUMENTATION PAGE

Form Approved OMB No. 0704-0188

1. AGENCY USE ONLY *(Leave blank)*	2. REPORT DATE September, 1994	3. REPORT TYPE AND DATES COVERED Master's Thesis

4. TITLE AND SUBTITLE
SOOT PARTICLE DENSITY DETERMINATION FROM A LASER EXTINCTION MULTIPASS TECHNIQUE (u)

5. FUNDING NUMBERS
N0042194 WR 01539

6. AUTHOR(S) Glaros, Gregory E.

7. PERFORMING ORGANIZATION NAME(S) AND ADDRESS(ES)
Naval Postgraduate School
Monterey CA 93943-5000

8. PERFORMING ORGANIZATION REPORT NUMBER

9. SPONSORING/MONITORING AGENCY NAME(S) AND ADDRESS(ES)
Naval Air Warfare Center Aircraft Division, Trenton, NJ 08628-0176

10. SPONSORING/MONITORING AGENCY REPORT NUMBER

11. SUPPLEMENTARY NOTES The views expressed in this thesis are those of the author and do not reflect the official policy or position of the Department of Defense or the U.S. Government.

12a. DISTRIBUTION/AVAILABILITY STATEMENT
Approved for public release; distribution is unlimited.

12b. DISTRIBUTION CODE
A

13. ABSTRACT *(maximum 200 words)*

Methods of measuring soot particle densities have been of interest for several decades. Plume signature determination of both rocket and air-breathing engines is of concern when applied to pollution and theater missile ballistic defense strategies. Application of non-intrusive traditional techniques employing Bouguer's law relied on Sauter mean diameter, statistical deviation and the probability density function in order to compensate for the ambiguities present in the extension of classical Mie theory. Our investigation developed an apparatus which will determine soot particle densities by measuring extinction from absorption of light energy transmitted through an exhaust plume. The method used was a two-pass technique using an optical phase conjugator (OPC) which returned the non-absorbed portion of light energy. When the apparatus was used with a retroreflector, it produced accurate results but did not compensate for thermal blooming or beam steering. Characteristics of a photorefractive crystal used in the OPC process allowed for the return of an incident beam corrected for aberrations. Although the OPC returned the phase conjugate of the incident beam its size precluded the return of all of the transmitted data because data was lost on the blossomed beam.

14. SUBJECT TERMS Soot particle density measurements, Phase conjugation, Barium titanate, Photorefractive crystals.

15. NUMBER OF PAGES 46

16. PRICE CODE

17. SECURITY CLASSIFICATION OF REPORT	18. SECURITY CLASSIFICATION OF THIS PAGE	19. SECURITY CLASSIFICATION OF ABSTRACT	20. LIMITATION OF ABSTRACT
Unclassified	Unclassified	Unclassified	UL

NSN 7540-01-280-5500

Standard Form 298 (Rev. 2-89)
Prescribed by ANSI Std. 239-18 298-102

Approved for public release; distribution is unlimited.

SOOT PARTICLE DENSITY DETERMINATION FROM A LASER EXTINCTION MULTIPASS TECHNIQUE

by

Gregory E. Glaros
Lieutenant , United States Navy
B.S., United States Naval Academy, 1986

Submitted in partial fulfillment
of the requirements for the degree of

MASTER OF SCIENCE IN ASTRONAUTICAL ENGINEERING

from the

NAVAL POSTGRADUATE SCHOOL
September 1994

Author: Gregory E. Glaros
Gregory E. Glaros

Approved by: Oscar Biblarz
Oscar Biblarz, Thesis Advisor

David W. Netzer
David W. Netzer, Co-Advisor

Daniel J. Collins
Daniel J. Collins, Chairman
Department of Aeronautics and Astronautics

ABSTRACT

Methods of measuring soot particle densities have been of interest for several decades. Plume signature determination of both rocket and air-breathing engines is of concern when applied to pollution and theater missile ballistic defense strategies. Application of non-intrusive traditional techniques employing Bouguer's law relied on Sauter mean diameter, statistical deviation and the probability density function in order to compensate for the ambiguities present in the extension of classical Mie theory. Our investigation developed an apparatus which will determine soot particle densities by measuring extinction from absorption of light energy transmitted through an exhaust plume. The method used was a two-pass technique using an optical phase conjugator (OPC) which returned the non-absorbed portion of light energy. When the apparatus was used with a retroreflector, it produced accurate results but did not compensate for thermal blooming or beam steering. Characteristics of a photorefractive crystal used in the OPC process allowed for the return of an incident beam corrected for aberrations. Although the OPC returned the phase conjugate of the incident beam its size precluded the return of all of the transmitted data because data was lost on the blossomed beam.

TABLE OF CONTENTS

ACKNOWLEDGEMENTS

I wish to thank my wife for her unfailing support and patience during this research. Without her support and love, this document would not exist. I also wish to thank Professor Oscar Biblarz and Professor David W. Netzer for their encouragement, support and guidance.

None of the laboratory work conducted for the completion of this research could have been done without the tireless patience and assistance of Mr. Harry Conner. He was responsible for some of the innovative techniques for the acquisition of the data. Also, the foundation for this research could not have been formed without the teachings of Dr. John Reintjes, Dr. Mark Bashkansky and Dr. Charles Askin, of the Naval Research Laboratory. These respected men devoted their unconditional attention to me during my experience tour discussing the principles of non-linear optics and optical phase conjugation. They have my endless gratitude and most sincere appreciation. I would like to also extend my appreciation to Mr. William Voorhees, of the Naval Air Warfare Center, Aircraft Division, who provided the funding for this research.

I. INTRODUCTION

The understanding of soot formation, the measurement of the resulting particle sizes and concentration together with the modelling of the plume signature for rocket and air breathing engines represent difficult problems which have been explored for several decades. Recent and increasing environmental concerns over pollutants emitted into the atmosphere as well as Defense Department concerns over plume signature continue to focus our attention on the need to determine emitted soot concentrations from air-breathing engines. The DoD is also concerned about the prediction of plume signature for theater missile ballistic defenses, a compelling challenge to the security of our forces.

The work reported here is a continuation of the approach followed by Biblarz and Netzer in their evaluation of optical measurements of turbine engine exhaust particulates. [Ref. 1] They reported that an "absorption coefficient", which is defined as the extinction cross section (q_e) divided by the particle mass (m_p), remains relatively constant with changes in wavelength and temperature.[Ref. 2] From this value and data provided by transmission measurements, soot mass concentration (i.e., the particulate mass loading of the plume) may be determined. The absorption coefficient μ_e results obtained for soot concentration, in this approach, agreed very well with those obtained using the theoretical extinction parameters based on Mie theory.[Ref. 1] Therefore, a practical instrument based solely on extinction measurements is being developed to measure the mass concentration of soot particles in exhaust plumes.

In gas turbine engine plume transmittance measurements, beam steering usually occurs, often resulting in low measured values of transmittance which are not caused by soot particles. These plumes also often have low obscurations. Accurate measurements are then difficult for a single-pass of light through the plume. The techniques employed in this investigation utilized a He-Ne (8mW) and an Argon-Ion (550mW) laser. The transmission was determined by passing monochromatic light through the exhaust plume twice, reflecting it off either a retroreflector or a photorefractive phase conjugate barium titanate crystal

($BaTiO_3$). The purpose of the latter procedure was to exploit the attractive properties of optical phase conjugation (OPC). Optical phase conjugation tends to correct for distortions arising from propagation through materials with poor optical quality (e.g, beam steering in plumes, thermal blooming, etc.). It recovers the aberrations but cannot recover absorption and scattering. Therefore, the ability to automatically retroreflect beams incident upon them along with the unique capability to produce an unaberrated beam, provides only the desired extinction or transmittance. Thus this "mirror" is ideally suited for extinction measurements.

The need to correct for thermal blooming and beam steering as well as the complexities of determining soot concentration caused the ambiguities present in the application of probability density functions extended to Mie scattering theories should be circumvented with the use of an optical phase conjugate mirror (OPM) together with the data reduction technique proposed in reference 1.

II. THEORY AND BACKGROUND

A. LIGHT TRANSMISSION TECHNIQUES

Soot concentration measurements have been based on both intrusive and non-intrusive techniques. Sampling (collection of particles on a filter or removal of smoke through a tube for external analysis) can distort the configuration of the particles in the medium and requires equipment which is difficult to build and calibrate.[Ref. 3] Some non-intrusive techniques utilize the definition of a SAE Smoke Number, and as such do not provide a quantitative measure of particulate density or a measurement of the sizes of the particulates.[Ref. 4] Other optical techniques have used multiple-wavelength extinction measurements and /or measurements of scattered light. [Ref. 5,6,7]

1. Principles of Extinction

Attenuation, or the extinction of light traversing a medium, is the result of both scattering and absorption of the energy from the source beam of light.

Extinction = scattering + absorption.

Therefore, the amount of light energy removed from the traversing beam directly indicates the extinction cross sections of the particles along the beam path. "The sun, for instance, is fainter and redder at sunset than at noon. This indicates an extinction in the long air path, which is strong in all colors but even stronger in blue light than in red. Looking sideways at the air, through which the sun shines, we see actually blue light is scattered more strongly," providing us with a red sunset.[Ref. 8] In this case extinction is caused by scattering and not absorption. For monochromatic visible radiation (from a laser) incident on soot, the dominant extinction occurs from absorption because of the highly absorbing soot. According to Mie calculations, the ratio of scattering to absorption for $x = 0.1$ is about 10^{-3} for soot (where $x = 2\pi a/\lambda$, a is the radius of the sphere, and λ = laser wavelength).[Ref. 9] Additionally, Van de Hulst points out that for absorbing particles the imaginary part of the complex refractive index m (where $m=n-in'$), varies from $n' > 10^{-8}$ for water to $n' \approx 1$ for metals in the visible range. For one-particle extinction, if I_0 is the intensity of the incident

light (watt/m^2), a given sphere will intercept $Q \cdot \pi a^2 \cdot I_0$ (watt) from the incident beam. Subsequently, the part absorbed and the part scattered in all directions can be found by replacing the extinction coefficient with either absorption or scattering.[Ref. 8] The transmission of the light beam can be expressed as $T = I / I_o$.

For the case of scattered light in directions away from the beam path, the energy lost is more dependent on particle shape, size, polarization of the incident light, and the index of refraction.[Ref. 10] For a wavelength of 500 nm and a particle diameter of 16 nm, the scattered intensity is rather minuscule when compared to absorption.[Ref. 1] In addition, for particles at a diameter of 1600 nm, the scattered and absorbed amounts are equivalent, but these equivalent spherical dimensions are out of the range of soot particles.

2. Bouguer's Law and the Extension of Mie Scattering Theory

As early as 1976 various researchers utilized the phenomena present in the attenuation of monochromatic radiation in order to obtain an optical, non-intrusive, continuous, *in situ* means of providing transmission measurements without disturbing the system.[Ref. 6] These measurements and the subsequent analysis were usually based upon Bouguer's law, also known as Lambert-Beer's Law, which states that the transmission of light through a cloud of uniform particles is given by :

$$T = e^{(-QAnL)} = e^{-(3QC_m \frac{L}{2\rho d})} \tag{2-1}$$

where;

- A - cross-sectional area of the particulate
- C_m - mass concentration of particles
- d - particle diameter
- L - path length containing the particles
- n - number concentration of particles
- Q - dimensionless extinction coefficient
- T - Transmittance
- ρ - particle density

However, Bouguer's law is only valid if the transmission measurements are made properly, i.e., the field of view of the detector must be narrow enough so that the amount of scattered light received by the detector is insignificant.[Ref. 7] Using Mie scattering theory for a single spherical particles, Q (the dimensionless extinction coefficient) can be calculated as a function of particle size, wavelength of light, and complex refractive index of the particle. This approach of course assumes that only independent scattering by particles is present, for example, the particles are considered sufficiently far from each other such that the scattering by one particle can be studied without any cooperative effect associated with other particulates.[Ref. 8]

3. Revision of Bouguer's Law for Polydispersions

A revision of Bouguer's transmission law by Dobbins, and consequently used successfully by Cashdollar, *et al,* showed that the transmission law for a polydispersion could be written in terms of the Sauter mean particle diameter (d_{32}) and mean extinction coefficient ($\overline{Q}$).[Ref. 11]

$$T = e^{\frac{-3\overline{Q}C_m L}{2\rho d_{32}}} \tag{2-2}$$

For two beams of different wavelengths passing simultaneously through the same plume;

$$\frac{\ln T_{\lambda_2}}{\ln T_{\lambda_1}} = \frac{\overline{Q_2}}{\overline{Q_1}} \tag{2-3}$$

Experimental Theory

where, $\overline{Q}$ is a function of $m=n-in'$, λ, and the assumed particle size distribution. The complex refractive index m contains the real part n, the index of refraction, the imaginary part

n', describes absorption, and λ is the wavelength. T_λ is a function of wavelength in the experimental process, and the values of $\overline{Q}$ are derived from theory. For example, if a log-normal size distribution is assumed to be present, d_{32} and σ_g (the geometric standard deviation) are sufficient to define the distribution. The unknowns are d_{32}, σ_g, n, and n'. Thus, a minimum of four independent ln-transmission ratios must be determined experimentally, but often many additional ratios are obtained. Variations of the four parameters are made until the best correlation with the theoretical extinction coefficient ratios is obtained.

This circuitous procedure requires multiple-wavelength measurements as well as a reliance on the assumed probability particle size distribution. Only if the complex refractive index, d_{32}, and the geometrical standard deviation are correct can the ratios be expected to yield the correct particle size. However, more than one particle size distribution is capable of providing an equivalent correlation. Once the correlation is obtained one value of T can be used to find the desired value of C_m. This multi-variable approach to obtain C_m is complicated at best and at worst susceptible to the inconsistencies always associated with probabilities, standard deviation, and the extension of classical Mie theory to include multiple non-spherical particles.

4. Defining Soot Measurements from an Extinction Parameter

The approach by Biblarz and Netzer, for the determination of soot concentration of exhaust particulates, is based upon a relative constancy for the extinction parameter μ_e. [Ref.1] A reference value of 5000 m^2/kg was selected based on the least variation in calculated aerosol density from the measurements of other investigators. Three wavelengths of 450, 630, and 1000 nm for carbon powders produced variations of approximately 5% when examined against data generated by Cashdollar [Ref. 7] and Few [Ref 5]. This technique resulted in similar findings by [Ref. 2] therefore, if the relative constancy of μ_e is correct, then it can be theorized that the lack of sphericity and the distribution of sizes do not greatly affect this value. When the extinction measurements are properly done (i.e., to exclude extraneous scattering and large particles) then the following equations will yield the mass concentration

of soot particles (ρ), assumed constant across the plume, and ultimately the soot mass flow rate $\dot{m}$, expelled from the combustor. The equations are:

$$\mu_e = q_e / m_p = q_e N / m_p N = \alpha / \rho \quad (2\text{-}4)$$

$$\mu_e \approx 5{,}000\ m^2 / kg \quad @\ \lambda \approx 0.450\ \mu m \quad (2\text{-}5)$$

$$T = \exp\{ -\alpha_e L_e \} = (I_B / I_o)/(I_P / I_o) \quad (2\text{-}6)$$

$$\alpha_e = (1/L_e) \ln (1/T) \quad (2\text{-}7)$$

$$\rho = (1/\mu_e L_e) \ln (1/T) \quad (2\text{-}8)$$

$$\dot{m} = \rho A V = A V \ln (1/T)/ (\mu_e L_e) \quad (2\text{-}9)$$

where;

α_e - extinction coefficient, turbidity, (units of inverse length)

A - cross-sectional area of the plume

L_e - extinction pathlength

N - total particle population density (particles per unit volume)

T - transmission ratio

V - mass-mean velocity

I_B / I_o - scene beam over reference beam intensity without particles

I_P / I_o - scene beam over reference beam intensity with particles

B. OPTICAL PHASE CONJUGATION

A major application of optical phase conjugation is in the correction of distortions arising from light energy propagating through materials with poor optical quality, such as the atmosphere, an optical filter, or in the present case an exhaust plume. The reflection from the crystal is accomplished by creating a complex conjugate of an electromagnetic wave. Fisher defines OPC as, " A technique that incorporates nonlinear optical effects to precisely reverse both the direction of propagation and the overall phase factor for each plane wave in an arbitrary beam of light."[Ref. 12] The distortion produced on propagating light energy through a medium can be seen in Figure 2.1 as:

Figure 2.1. Planar wave aberrated by a distorting medium.

From this depiction it can be seen that a plane wave develops considerable structure after passing through the aberrating material. If on the other hand we know how the medium will distort the wave front then the process can be reversed. The end product would be the original undistorted planar wave, as illustrated below.

Figure 2.2. Distorted wavefront corrected to planar form.

Mathematically, this corresponds to a wavefront that is the complex conjugate of the original plane wave. The approach depicted above in Figure 2.2 is used in adaptive optics

where the light source is independent of the termination point, such as in modern telescopes, in order to compensate for atmospheric aberrations. In the present application a phase conjugate mirror is utilized. The OPC mirror reflection conjugates both normal and tangential components, whereas an ordinary mirror conjugates only the normal component.

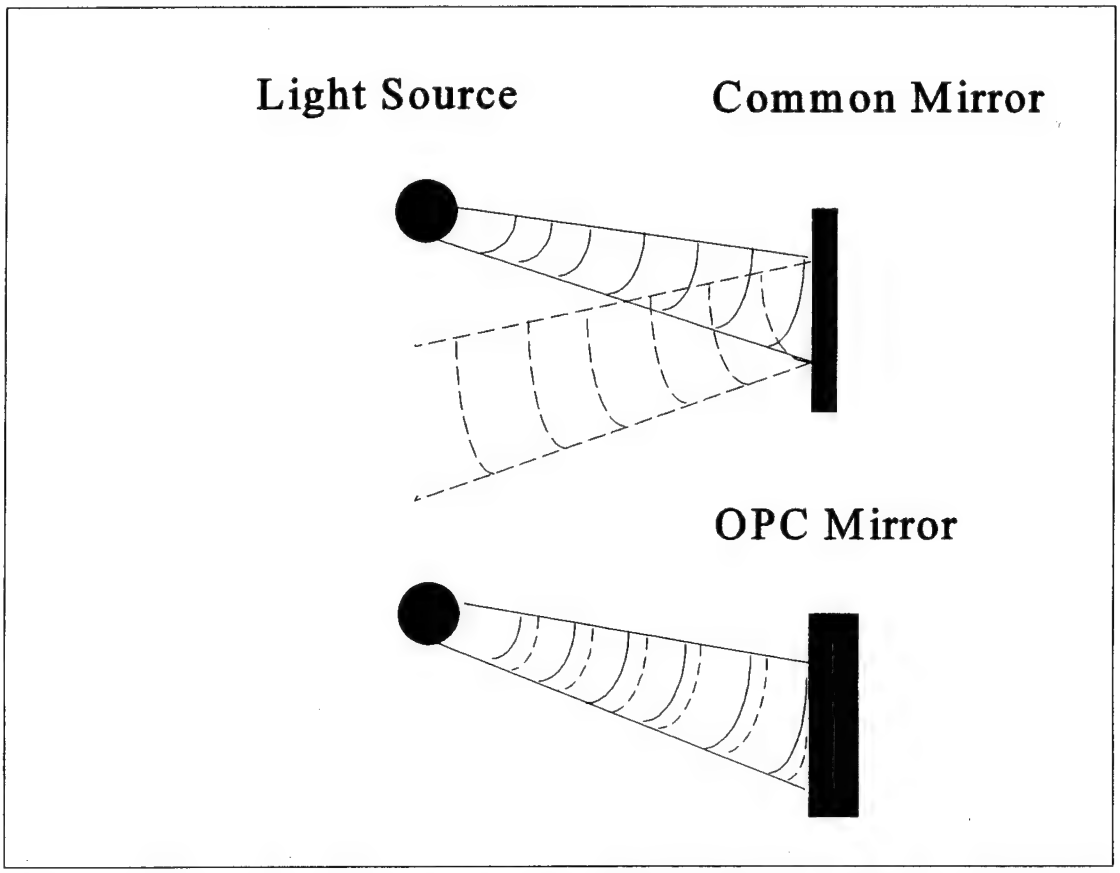

Figure 2.3. Comparison of a spherical wave reflection from an ordinary mirror and a phase conjugate mirror.

In mathematical terms the reverse propagation of a conjugate beam can be seen by considering an optical wave propagating through a linear lossless, distorting medium in the +z direction.

The electric field $E_1(r,t)$ is:

$$E_1(r,t) = RE[\psi(r)e^{i(\omega t - \kappa z)}] \tag{2-10}$$

The dependence of ψ on r reflects the spatial information it carries and the effects of distortion. If an optical field $E_2(r,t)$ is generated in such a way that the real part of $E_2(r,t)$ is the complex conjugate of the spatial part of $E_1(r,t)$ then the wave is called the phase conjugate of $E_1(r,t)$, such that;

$$E_2(r,t) = RE[\psi^*(r)e^{i(\omega t + \kappa z)}] \tag{2-11}$$

The reflected wavefront of $E_2(r,t)$ coincides everywhere with those of $E_1(r,t)$ with the only difference being that it propagates in the reverse direction.[Ref. 13] This conjugate processing of E_1 is commonly known as 'time reversal'.

Using the properties of OPC yields a restored unaberrated phase front after it has passed twice through the same distorting medium, e.g., the exhaust plume. The illustration below depicts this process of distortion correction by a Phase Conjugate Mirror (PCM).

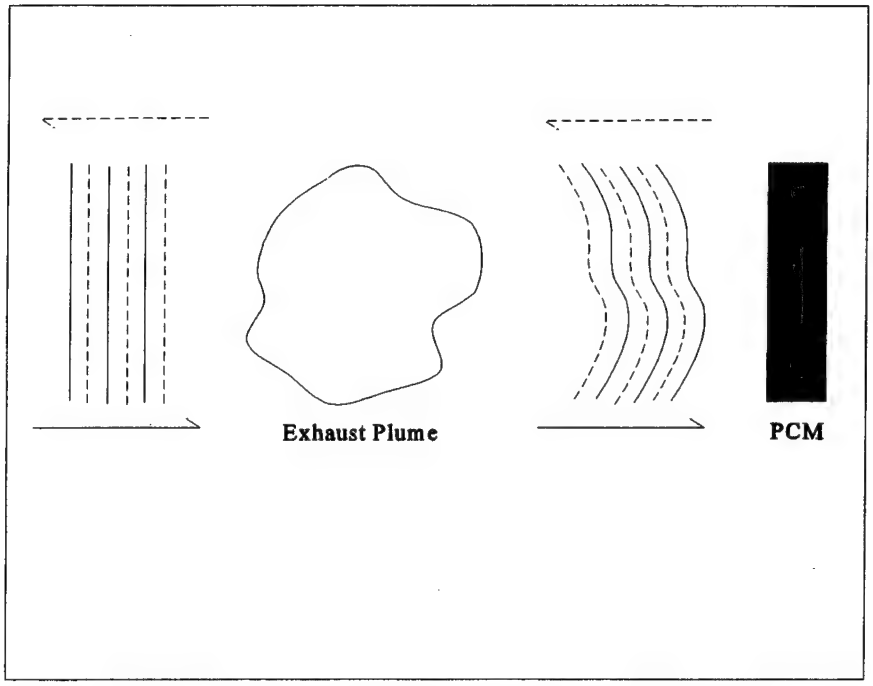

Figure 2.4. Illustration of aberration correction by a phase conjugate mirror.

From this process it can be seen that the depleted light intensity data returned through the OPC will result in little or no disturbances, except for extinction. Therefore, the transmittance can be directly determined from the resulting intensity ratios.

1. Photorefractive Effect

An explanation of the photorefractive effect in electro-optic materials is predicated on the existence of charges in a crystalline materials as first proposed by Chen (1969).[Ref.12] According to Fisher the charges in the crystal are located in low-lying traps formed by impurity or defect sites.[Ref. 12] In the presence of light energy, these trapped charges are held in place by the small dark conductivity of the crystal. Gunter also explains that this photoexcitation of free carriers diffuse or drift in an externally applied electric field away from the light energy to these trapping sites.[Ref. 14] This redistribution of charges creates an electrostatic field within the nonlinear medium in the illuminated volume of the crystalline structure. In addition, this space charge field also generates a change in refractive

index by the linear electro-optic effect. The light induced electrostatic field can be on the order of 10^5 V/m, which will cause a change of the refractive index (10^{-3}) in materials such in $BaTiO_3$ (which possess large linear electro-optic coefficients).[Ref. 12] This photorefractive effect is dependent on the material and may be induced by ultraviolet, visible or infrared radiation.[Ref. 14]

The details of the photorefractive effect summarized by Fisher can be described as a three step process.

1. Light causes charge to migrate and separate in a crystalline material.
2. The separation of charge produces a strong electrostatic field.
3. The electrostatic field then causes a change in the refractive index of the crystal by the linear electro-optic effect.

It should be noted that the photorefractive effect on index change is independent of the total intensity of the incident beam. Although the speed with which the process exists does rely on total light intensity. Even a small beam intensity of milliwatts or microwatts (Huignard *et al*, 1979; Feinberg *et al*, 1980; Feinberg and Hellwarth, 1980) can produce optical phase conjugation in photorefractive materials such as $BaTiO_3$ using another process called four- wave mixing. The simplicity of 'self-conjugation' with a single laser is more desirable than four-wave mixing because of alignment complexities and because four-wave mixing can produce a reflectivity greater than one.

2. Model of an Optical Phase Conjugator

A model is presented to describe the phenomenon of OPC using photorefractive materials. The photorefractive material itself contains certain types of impurities or imperfections. These ionized impurities are capable of capturing electrons. In addition, the rate of electron generation is $(sI + \beta)(N_o - N_o^i)$ and the trap capture is $\gamma_R N N_D^i$.

N - electron density

N_D - density of donor impurity

N_D^i - density of ionized donor impurity

s - cross section for photoexcitation

β - rate of thermal generation of electrons

γ_R - electron-ionized trap recombination rate

The rate equation for N_D^i is written as:

$$\frac{\delta N^{i_D}}{\delta t} = sI(N_D - N_D^i) - \gamma N N_D^i \tag{2-12}$$

The generation rate of electrons is the same as that of the ionized impurities except that the electrons are mobile and the impurities are stationary. Therefore, the rate equation for electron density can be written as:[Ref. 15]

$$\frac{\delta N}{\delta t} - \frac{\delta N^i{}_D}{\delta t} = \frac{1}{q} \nabla \cdot j \tag{2-13}$$

The current density j consists of contributions from the drift of charge carriers and diffusion, which results from the gradient of carrier density. The current density equation is as follows:

$$j = qN\mu E + k_B T \mu \nabla N \tag{2-14}$$

μ - mobility factor;

E - electric field;

$k_B T$ - product of Boltzman's constant and Temperature.

This electric field E will obey Maxwell's equation defined as:

$$\nabla \cdot \varepsilon E = \rho^{(r)} + -q(N + N_A - N^i{}_D) \tag{2-15}$$

where; ε - permittivity

$\rho^{(r)}$ - charge density

N_A - density of acceptor impurity

In the absence of light illumination the charge neutrality can be written as:

$$(N + N_A - N^{i}_{D}) = 0 \qquad (2\text{-}16)$$

where if N is small, then $N_D^i = N_A$ in the absence of light.[Ref. 16]

When the photorefractive material is illuminated, bright regions will be formed by the absorption of photons. Dark regions will be formed by the trapping of the remainder of positively charged ionized donor impurities. This process then leads to the above mentioned charge separation which will induce an electrostatic field.

3. Barium Titanate

Barium titanate is classified as an oxygen-octahedra ferroelectric photoconductive single-domain crystal. Of the many photorefractive gain materials available $BaTiO_3$ has the most desirable combination of high exponential gain coefficient Γ with comparatively low optical absorption ($\alpha \approx$ 1-2/cm at 514.5 nm).[Ref. 17] Ford, *et al,* have demonstrated signal gains as high as 4000 and a Γ of 22 cm^{-1} for conventional $BaTiO_3$ without the use of externally applied field of a frequency shifted pump wave. From the gain equation below it is evident that a small increase in Γ will increase G considerably.

$$G = \frac{I_{out}}{I_{im}} = \frac{(1+r)\exp(\Gamma L)}{1+r\exp(\Gamma L)} \qquad (2\text{-}17)$$

r - signal / pump intensity ratio

L - interaction length

A disadvantage of the Barium Titanate crystal is the requirement for acute beam incident angles to produce high gain coefficients. This is a result of the high index of refraction (≈ 2.4) in comparison with air, which refracts the input beam at the input face. To resolve this matter as well as the resultant reduction in the effective input aperture of the crystal and an incomplete utilization of the crystal volume, Ford, *et al,* proposed in 1984 to cut the $BaTiO_3$ crystal input face at 45° to the optic axis *C*.

4. Improved Performance of a 45° -cut

In Pepper's studies, improved performance over the conventional 0° -cut crystal went from 50% reflectivity to 62% using a 45^0 -cut, and corrected for specular reflection losses to ~ 73%.[Ref. 18] Further more Ford, *et al*, documented an increase in the response time of one order of magnitude greater than in the 0° -cut.[Ref. 17]

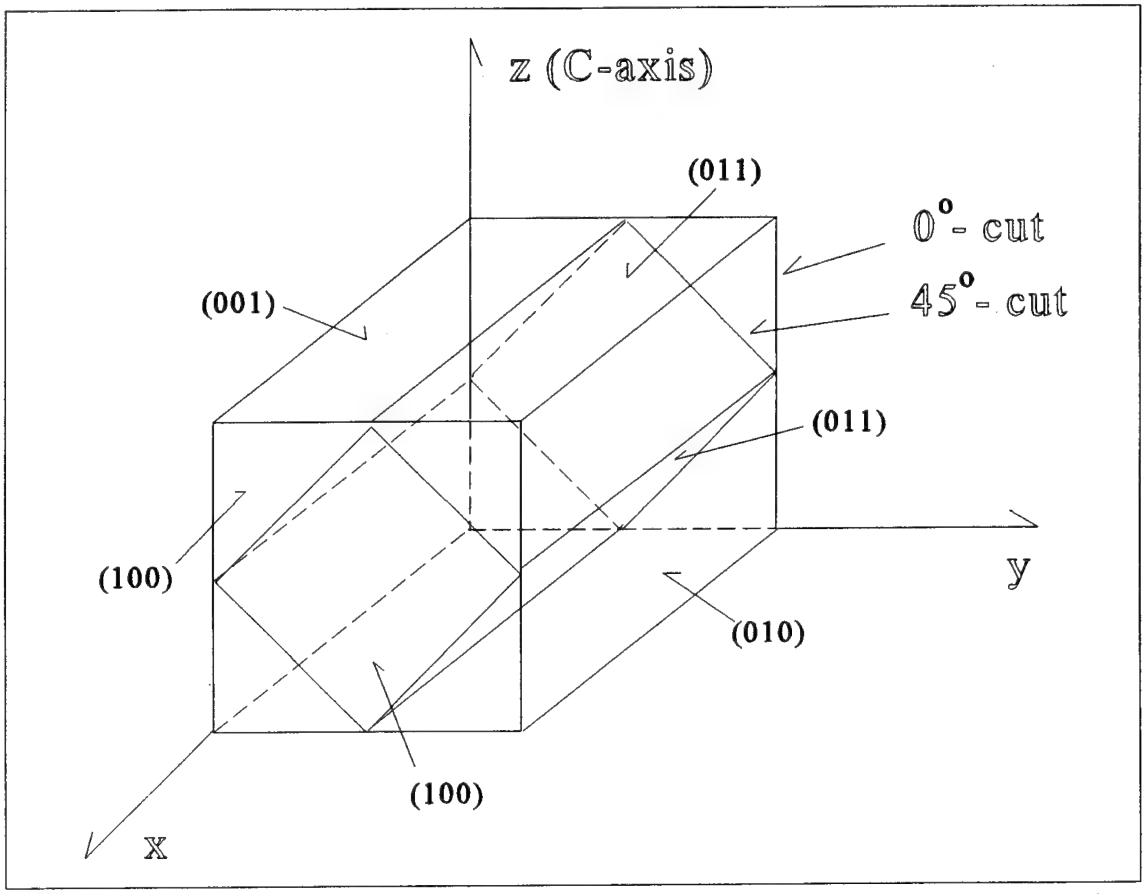

Figure 2.5. Orientation of the 45° - cut $BaTiO_3$ crystal (with faces on the (100), (011), and (011) crystalograhic planes) relative to the 0° - cut crystal. After[Ref. 16]

5. Evolution of the Light Scatter Patterns

Photographs illustrating the evolution of a phase conjugate output from barium titanate were reported by Brody and Goff .[Ref. 19] As the initial beam passes through the crystal, except for the effects of specular reflection, refraction, and some scattering, it is at its peak throughput. The beam then begins to fan (forward scattering of the input beam) toward the C axis corner. This is thought to be caused by intrinsic inhomogeneities by volume phase gratings produced photorefractively from the interference of the input beam and the weak scattered light.[Ref. 20] The initially transmitted intensity begins to diminish as the phase-conjugate output power begins to rise. At this point a transmission grating is forming with some of the input deflected to the back corner of the crystal, which returns light energy as back-propagating output. With an efficient steady phase conjugate fully developed diminution of the throughput is complete. The mature pattern internal to the crystal will show that most of the intrinsically scattered light will emanate from the forward region of the pattern near the crystal input.

III. EXPERIMENTAL INVESTIGATION

A. OVERVIEW

The objective of the experimental work was to demonstrate the application of two-pass transmission measurement for the determination of soot particle concentrations in plumes in the presence of noise/vibrations. The plume employed was that of a liquid fuel ramjet operated near stoichiometric with cold inlet air. Two methods were utilized; one in which the returning laser energy was provided by a retroreflector, and the other where a $BaTiO_3$ optical phase conjugator was utilized. These transmission data were also compared to those obtained using a front-surface mirror for reflection depicted in the next section as Figure 4.1.

1. Setup

In the test cell environment, low and high frequency vibrations (acoustic and mechanical are often present. It is therefore often necessary to obtain the transmittance measurements (I and I_o) at high speed because variations in I_o can often occur during the test.

Diagrams of the experimental layouts can be seen in Figures 3.1, 3.2, and in the next chapter as Figures 4.1, and 4.5. The lasers used are a 8 mW HeNe laser for the retroreflector (Fig.3.2) and a Lexel Model 95 Argon Ion laser with an output power of 550 mW at 514.5nm for the photorefractive crystal (Fig. 4.5). The Argon Ion lasers polarization was adjusted to provide the crystal with linearly polarized light to the C axis displayed in the last section as Figure 5.1, and incident on the (011) crystalographic plane for maximum phase conjugation (Fig. 2.5). A shutter was used to provide for the sequential input of the incident beam to the scene beam on the photodiode. This process provided an accurate means of determining the extinction ratio directly during each run (equation 2-6). I_B / I_o is obtained without particles present and is the "reference" ratio that corresponds to T=1.0. Initially, a liquid crystal shutter was utilized but was later replaced with a mechanical shutter with a peak frequency of 4000 Hz. The replacement was required because of the liquid crystal's inability to completely extinguish the incident beam energy from the photodiode. Additionally, the amount of light leak through was dependent on the intensity of the lasers throughput and, as a result, was

not linear. Therefore, a tare value could not be accurately determined and this resulted in inconsistent values for I_o. Although the mechanical shutter provided true zero values for I_o it was limited to only 4 kHz, as opposed to the nearly 20 kHz of the liquid crystal shutter. In an actual test cell application a much higher chopping frequency will be required.

The recorded signals, I_B, I_P and I_o were detected by a 400 Ghz photodiode. The data were then recorded by a 486 33MHz PC using Viewdac data acquisition system software, and analyzed with Lotus 123 spread sheet. Four thousand (4000) samples were collected at 250,000 samples per second. This provided a 0.2 second snapshot of the ramjet's sooty plume.

Once the chopped-signal technique was observed to work properly using the retroreflector, the phase conjugate crystal was utilized. Difficulties arose due to coupling of the conjugate wave with the laser cavity which cause power fluctuations in the laser cavity and degradation of the conjugate beam.

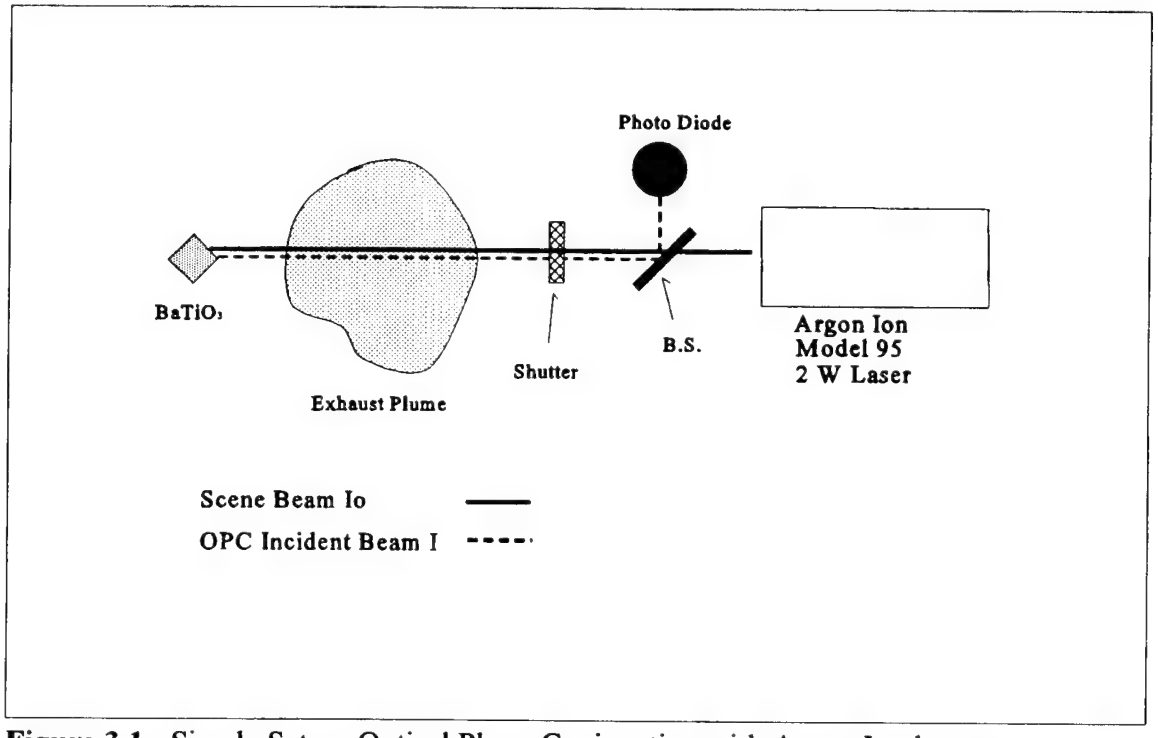

Figure 3.1. Simple Setup, Optical Phase Conjugation with Argon Ion laser.

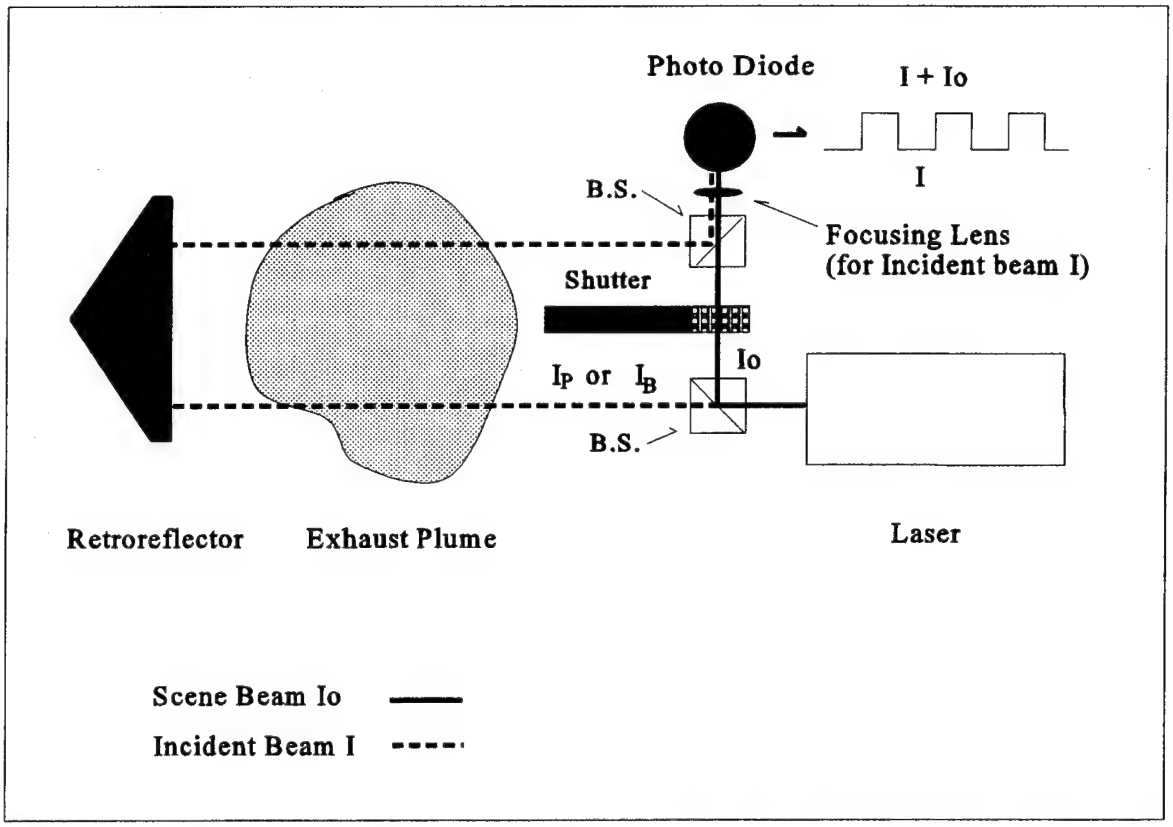

Figure 3.2. HeNe laser incident on retroreflector.

2. Procedure for the use of the Chopped Signal and Data Acquisition

After the laser was energized, the mechanical shutter stabilized to 4000 Hz, and the optics were adjusted, a first run was made in order to obtain I_B / I_o without particles present. The square wave generated is a result of the input of the incident and scene beams at the top of the wave with just the scene beam appearing at the bottom of the signal (Fig. 3.2 photodiode). I_B and I_o were then derived using Lotus 123 spread sheet. When the laser passed through the exhaust plum of the ramjet, values of I_P / I_o were obtained at 4000 Hz. A post-run was then made to determine if I_B / I_o had remained constant. T was then calculated versus time from the ratio $(I_P / I_o) / (I_B / I_o)$.

IV. DISCUSSION OF RESULTS

A. INTRODUCTION

The sequence of testing was an incremental approach designed to validate each step of the experimental process. The ability of the apparatus depicted in Figure 3.2 to obtain accurate transmittance data was first proven by comparing its output to a simple setup of passing the incident beam through the exhaust plume and returning it by a common mirror to a diode (Figure 4.1). These runs were conducted using an 8 mW He-Ne laser. The next step was to operate the apparatus shown in Figure 4.5 (part two, Argon-Ion results) using the optical phase conjugating barium titanate crystal , and compare the obtained results again with the data from the simple mirror setup. A video recorder was mounted beneath the plume so that the plume dimensions (L_e, equations 2-7, 2-8) could be determined.

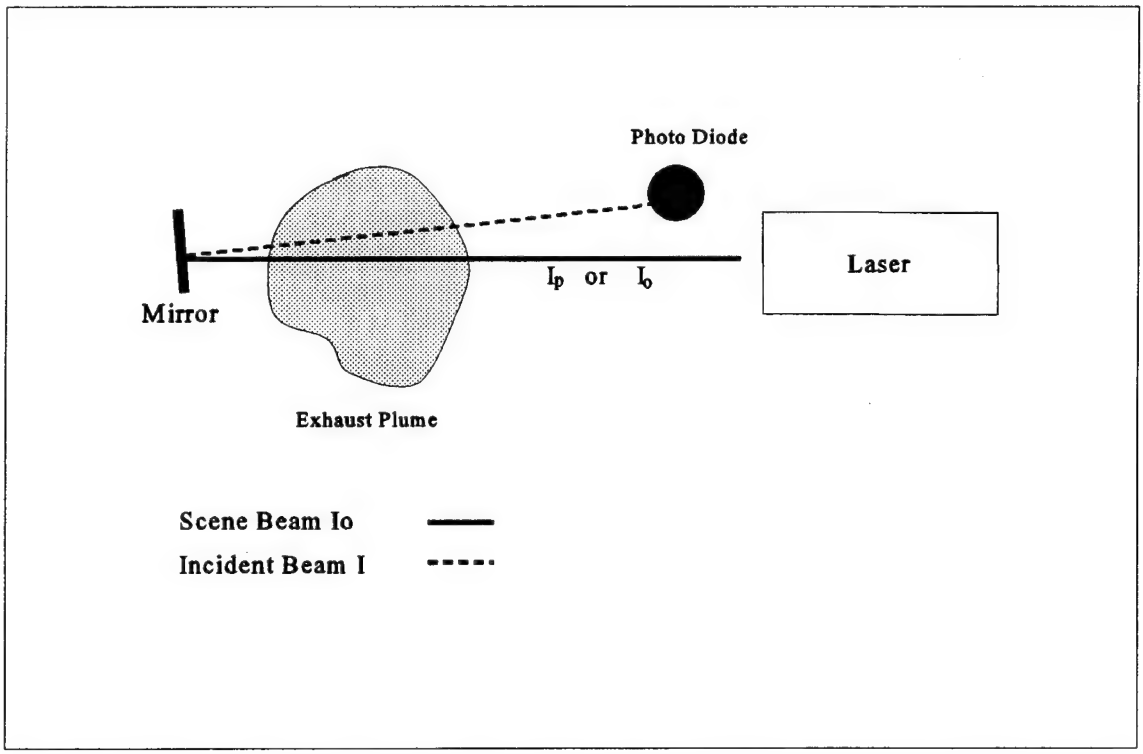

Figure 4.1. Simple Setup, Common mirror with HeNe or Argon Ion laser. I_o measured before the run, and I during the run, producing $T = I_P / I_o$.

B. SUMMARY OF FINDINGS

Table 4.1 lists the results obtained for transmittance of He-Ne and Argon-Ion lasers through an liquid fuel ramjet's exhaust plume.

RUN	LASER run type	PRE I Io	RUN I Io	POST I Io	T_R %	L_ex2 (m)	ρ kg/m^3
1	HeNe	0.838	0.387	0.800		0.412	
	fig. 3.2	3.632	3.634	3.611	0.471		3.66E-4
2	HeNe	0.437	0.271	0.480		0.390	
	fig. 3.2	2.504	2.506	2.452	0.613		2.51E-4
3	HeNe	0.530	0.262	0.504		0.412	
	fig. 3.2	3.510	3.514	3.451	0.502		3.35E-4
4	HeNe	0.731	0.537	inval		0.304	
	fig. 3.2	0.766	0.827	inval	0.680		2.53E-4
5	HeNe	N/A	2.037	N/A		0.304	
	fig. 4.1	4.008	N/A	3.962	0.511		4.41E-4
6	Argon Ion	N/A	0.817	N/A	0.177	0.304	8.31E-4
	fig. 3.1	4.689	N/A	3.894	0.28*		
7	Argon Ion	N/A	0.855	N/A	0.185	0.304	7.99E-4
	fig. 3.1	4.77	N/A	4.453	0.30*		
8	Argon Ion	N/A	0.947	N/A	0.531	0.304	4.17E-4
	fig. 4.1	1.801	N/A	1.771			

Table 4-1. HeNe and Argon Ion soot particle density extinction experimental runs.

* Indicates correction factor due to beam spot size/crystal ratio

1. He-Ne Results with Chopped Signal

Experimental runs 1-5, using the He-Ne with the designed optical apparatus and the common mirror, shows transmittance values ranging from 0.47 to 0.68. The calculated mass concentration of soot particles, ρ, was between 2.51 and 3.66E-4 (the common mirror approach yielded a lower transmittance). This result could be from the thermal blooming as well as beam steering effects on the incident beam. The diverging beam aberrated by these effects in the distorting medium of the exhaust plume exceeded the dimensions of the diode window, thereby causing it to lose some of its incident energy.

Variations in the actual transmittances were mainly a result of differing test conditions, i.e., differing air-fuel ratios used in the ramjet. In all but the forth run, the system extracted the same or nearly constant values for I_o. Some pre-run, post-run shift in I (particularly in run 2) must have been due to dirty optics and or a shift in the retroreflector. The apparatus showed that for most of the runs the system was stable and that the resultant degradation in the incident beam I was a result of the distorting medium (exhaust plume) and not the apparatus. The forth run indicated a movement in the system caused by the ramjet's acoustic vibration. The movement was such that the data collected for the post-run were ruled invalid. This run also revealed movement during the run by comparing run data I_o to pre-run I_o.

The conclusion derived from these findings was that the apparatus can indeed give a good value of transmittance (although uncorrected for thermal blooming, beam steering, etc.) through the exhaust plume. A comparison in the loss of energy by extinction is made in Figure 4.2, with Pre-Run and Run data superimposed. Figures 4.3 and 4.4 below show the chopped data created by the Figure 3.2 system setup. Pre-Run, Run, and Post-Run data were collected with $I + I_o$ at the top of the square wave and I at the bottom.

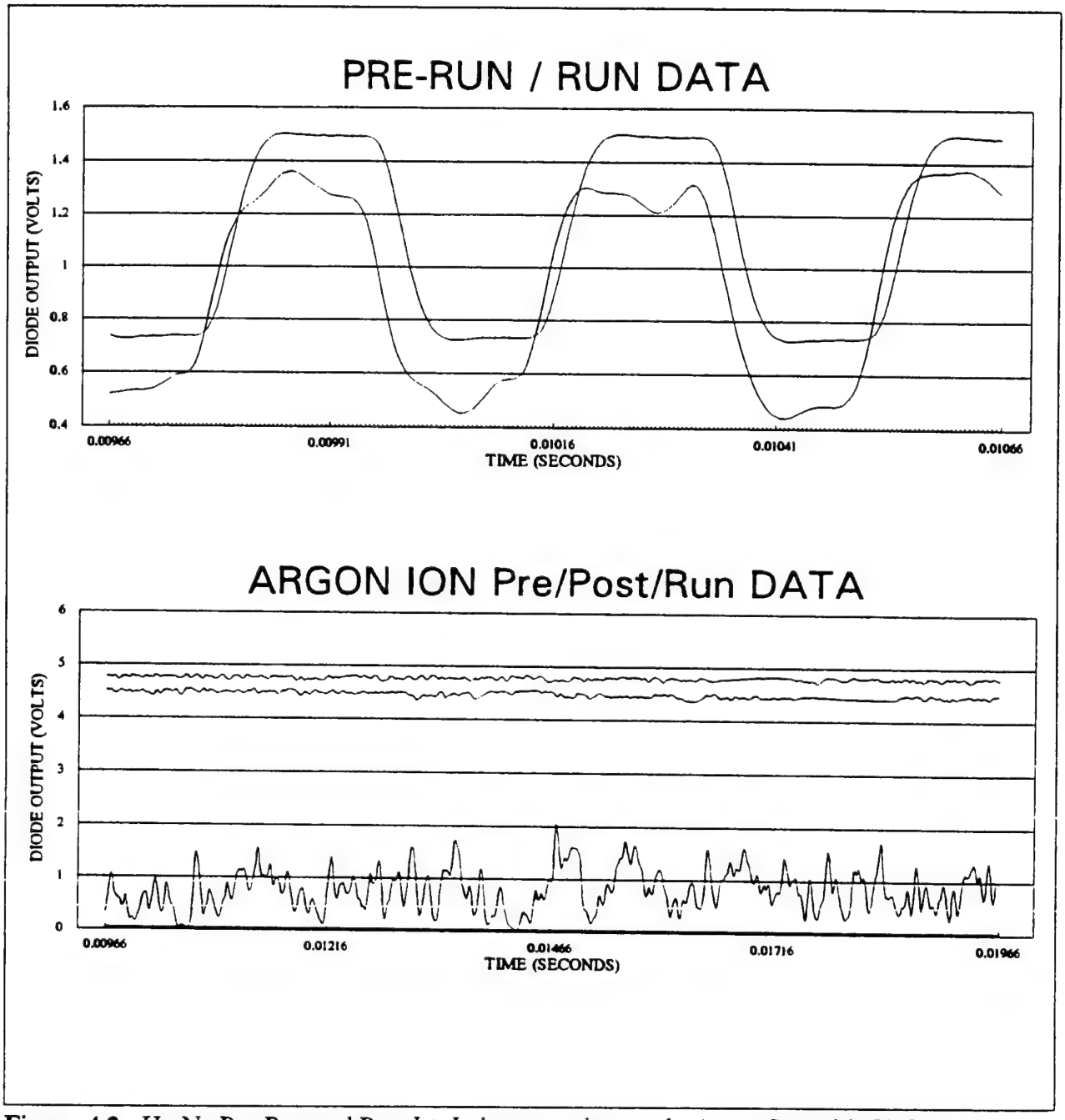

Figure 4.2. He-Ne Pre-Run and Run $I + I_o$ data superimposed. Argon-Ion with OPC barium titanate crystal, Pre-Run, Post-Run, and Run data superimposed (I and I_o).

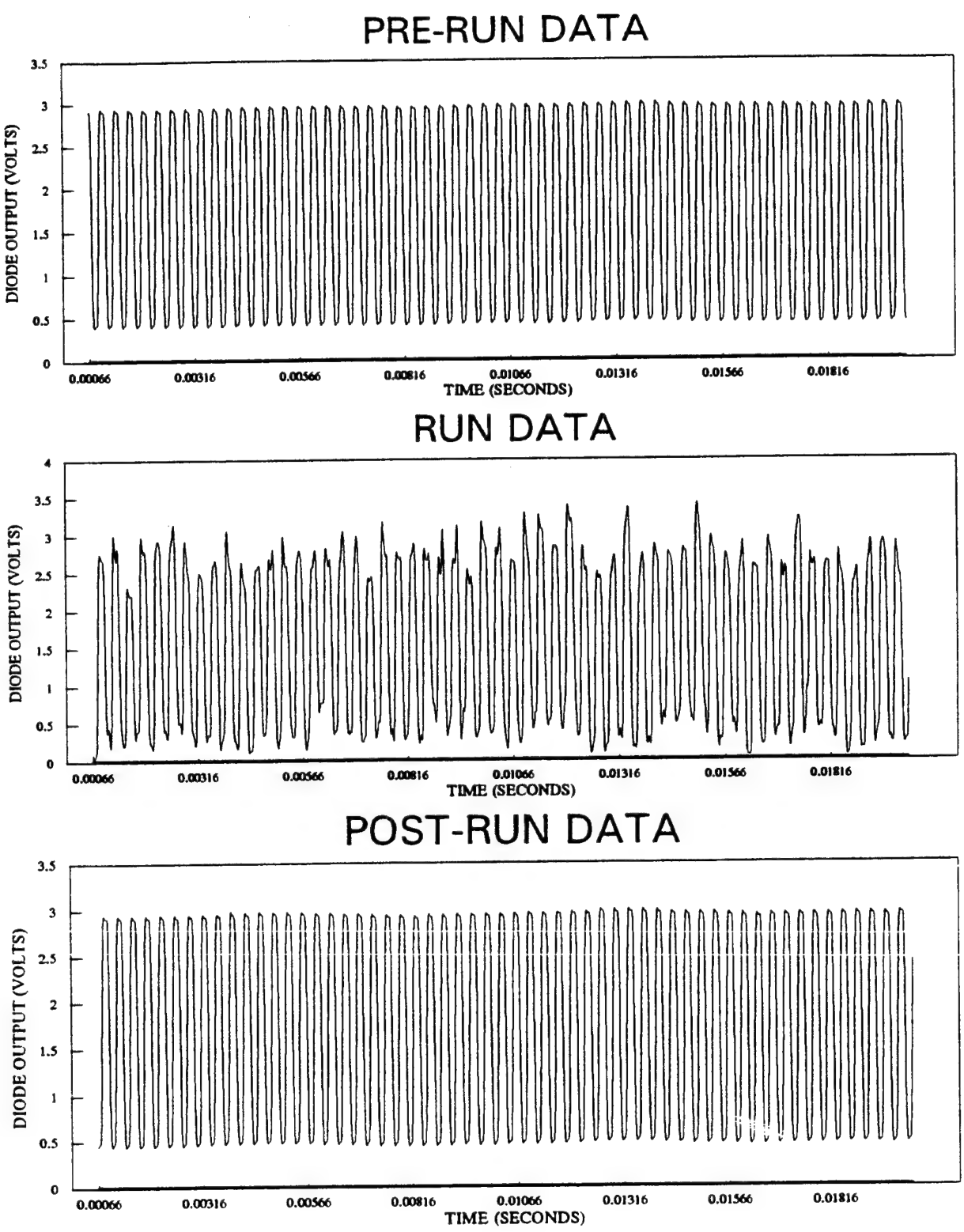

Figure 4.3. He-Ne Pre-Run / Run / Post-Run data using figure 3.2 apparatus.

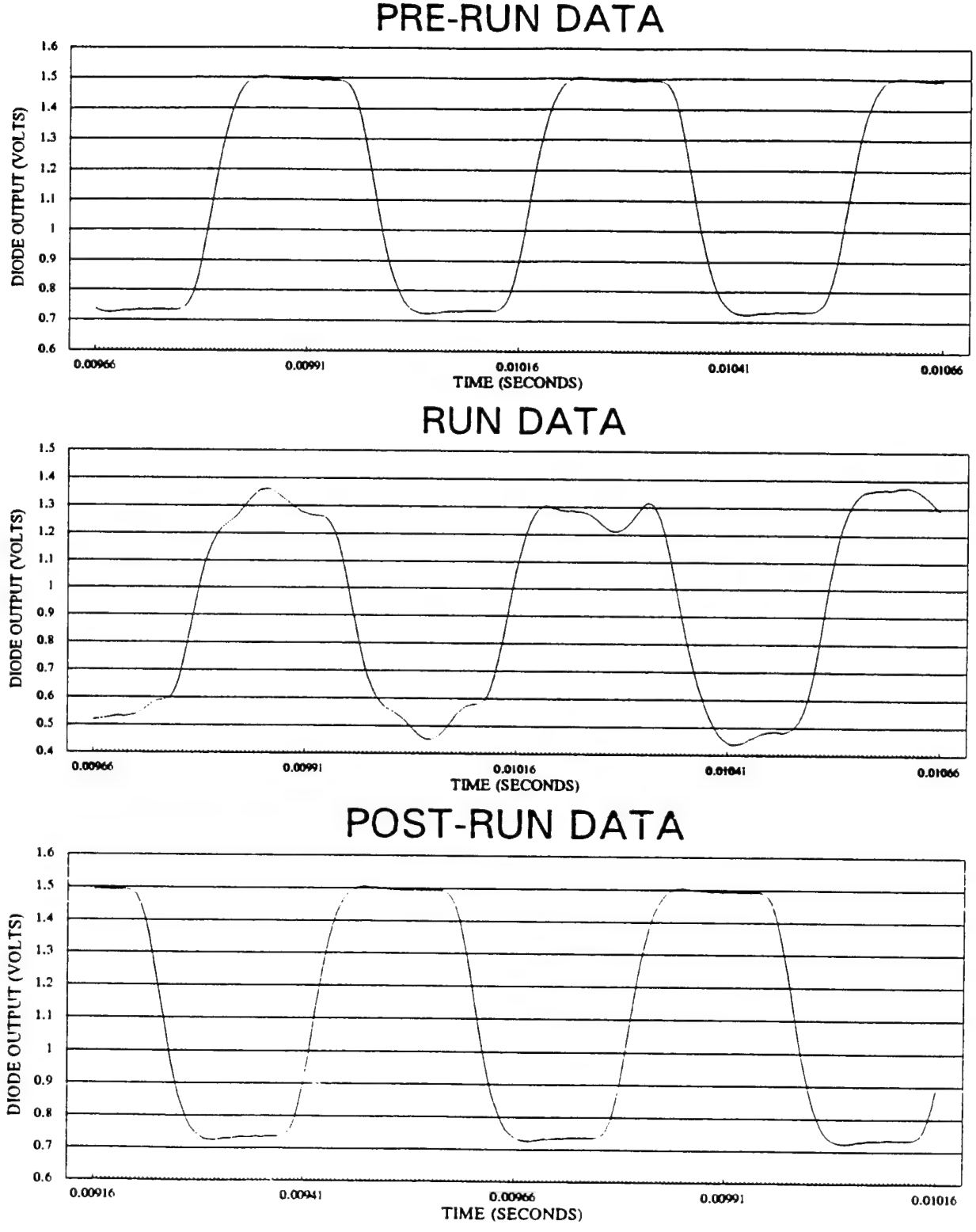

Figure 4.4. He-Ne Pre-Run / Run / Post-Run data expanded using figure 3.2 apparatus.

2. Argon-Ion Results

The 10 mW Argon-Ion used initially with the system configured in Figure 4.5 was not powerful enough to compensate for the losses imposed by the beam splitters. These losses prevented the required conjugate threshold in the barium titanate crystal from being reached. In addition because of the dimensions of this laser, alignment could not be accurately accomplished. A Lexel Model-95, 2 W, multi-mode, linearly polarized, Argon-Ion Laser tuned to 550 mW, was then used. Although this laser had ample power available, its dimensions also prevented the use of the chopped signal apparatus. Therefore a simple laser, beam splitter, and conjugate crystal setup was used to obtain the transmittance (Fig. 3.1).

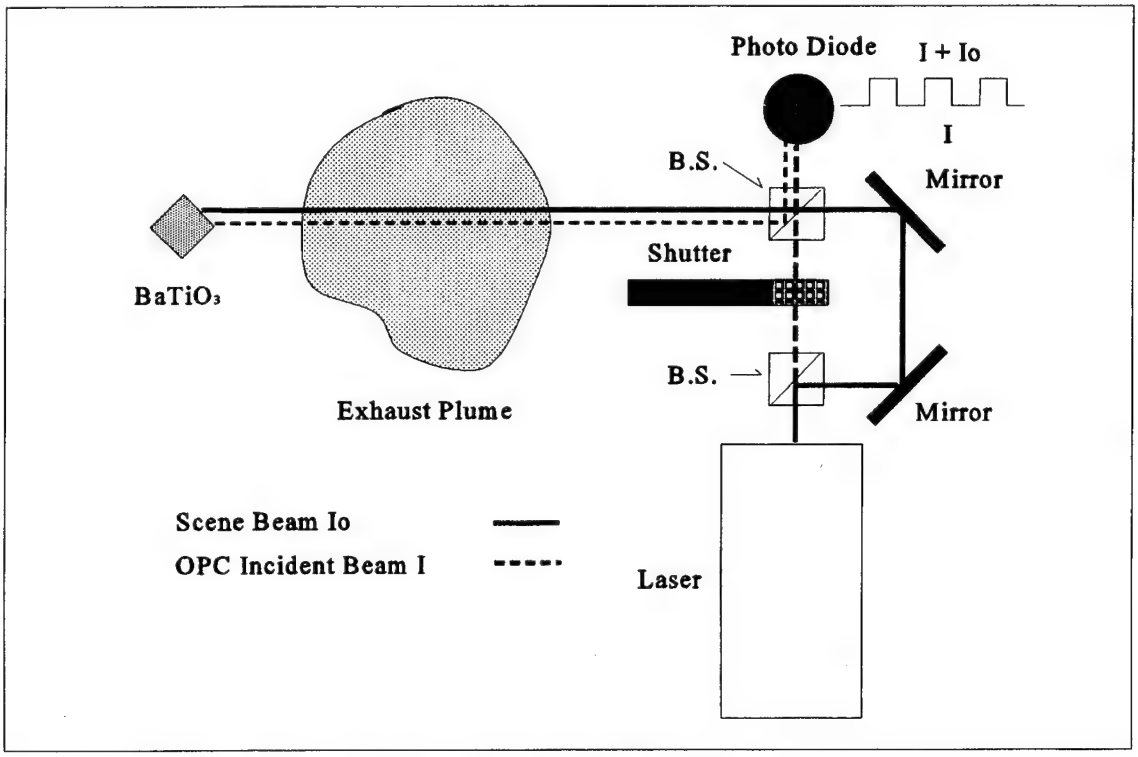

Figure 4.5. Optical Phase Conjugation with Argon Ion laser.

A manually actuated electric shutter was placed in the beam path. This was required because, without a Faraday rotator, phase conjugate energy returned into the laser cavity, causing unpredictable power fluctuations, and after approximately 40 seconds, loss of the conjugate beam. Because of the high power of this laser, operated at 550 mW, conjugation occurred almost simultaneously with open actuation of the shutter. With the shutter open and no plume present I_o was obtained, with the shutter again opened but with a plume present, I_P could be obtained. This, of course, did not compensate for vibration induced changes during the test, but the purpose at this point in the investigation was to see if the conjugate would return transmittance data.

In Table 4.1, runs six through eight were made using the Figures 3.1 and 4.1 system setup. It is clear from the transmittance data given in runs six and seven (Fig. 3.1) that consistent values of transmittance were produced by the phase conjugate crystal, despite the manual shuttering process. It is also clear that the transmittances produced by the barium titanate crystal were significantly lower, ~ 0.18, when compared with run 8 in which the mirror was used.

A video camera was then placed on the mirror, which replaced the photorefractive crystal for run eight. The intent was to see how much thermal blooming and beam steering occurred when it passed through the exhaust plume. The result was that the beam spot size increased 56 % in area. This created a beam spot size which exceeded the small dimensions, 4.5 mm cube, of the barium titanate crystal. The original beam spot size on the crystal was 3.8 mm. This essentially filled the volume of the crystal which produced a phase conjugate return. With the beam blooming to 5.7 mm, light energy incident on the crystal was obviously lost. If it is assumed that 56 % of the energy was lost (a uniform beam intensity), then a correction factor of 1.56, multiplied by the transmittance ratios of runs six and seven, would be needed. This resulted in "corrected" transmissions of approximately 0.30. Although the present apparatus did not permit accurate transmittance data to be obtained the concept of using a phase conjugate crystal was successfully demonstrated in the plume environment.

V. CONCLUSIONS AND RECOMMENDATIONS

The apparatus using the retroreflector is capable of making accurate multi-pass transmittance measurements in plumes. However, vibration hardening of the equipment will be required. In addition, beam steering and thermal blooming remain a problem.

In order to improve the utilization of the OPC apparatus in a test cell environment, the following must be accomplished:

1. Add a Faraday rotator or other optical isolator device.
2. Use a single frequency operating laser - etalon placed in the laser cavity.
3. Provide Argon-Ion laser power >> 10 mW or equivalent laser.
4. Incorporate a four-pass, vibration-free OPC unit.

The $BaTiO_3$ crystal will only conjugate with vertically and linearly polarized monochromatic light energy, oriented correctly toward the *C* axis, as shown below.

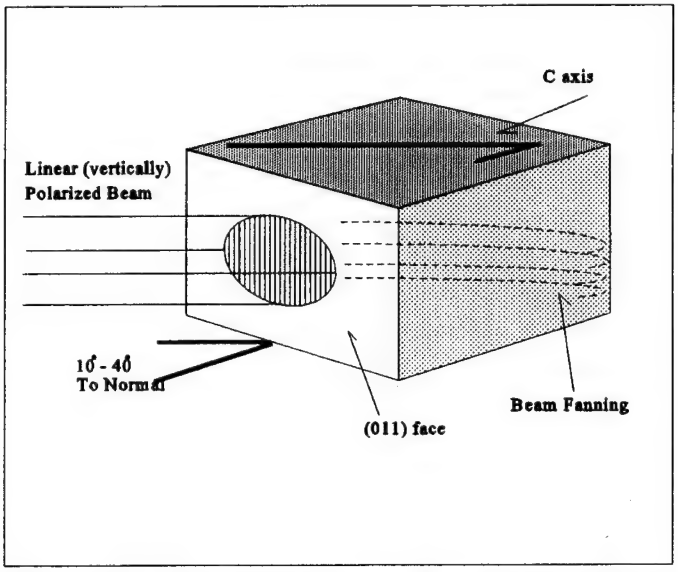

Figure 5.1. Direction of incident beam on a 45° cut $BaTiO_3$ crystal.

Although not absolutely necessary, this incident light should be extraordinarily linearly polarized. This can only be achieved with a Faraday rotator, placed in front of the exiting laser beam. In addition to linearly polarizing the light energy, the Faraday rotator also prevents the conjugate beam from retracing its path back into the laser cavity. Without this optical protection the laser power output will pulse, fluctuate, and create a interference grating with the incoming incident OPC. With a more powerful laser, this can and will result in damage to the laser itself. An alternative might be to chop the scene beam light at a frequency that maintains phase conjugation while preventing laser power oscillations.

Secondly, $BaTiO_3$ or any photorefractive crystal demands single frequency incident light to optimally conjugate. That is, the incident beam should be only a first order, Transversing mode (TEM_{01}). The following explanation is provided by Lexel Manufacturing.

> "The output of a laser operating on a single wavelength has a very narrow linewidth and extremely good coherence compared to any other type of light. However the laser line is actually made up of a large number of longitudinal modes spaced over a frequency bandwidth of approximately 5 Ghz. These longitudinal modes are related to the distance between the two mirrors making up the optical cavity. The frequency spacing between these longitudinal modes is c/2L, where c is the velocity of light and L is the mirror spacing. Thus a 1 meter cavity length has a 150 Mhz longitudinal mode spacing.
>
> The coherence length, i.e., the path distance over which the laser wavefront remains in phase and usable for interferometric effects, is approximately given by $c/\Delta\nu$ where $\Delta\nu$ is the frequency bandwidth of the laser line. The normal multi-longitudinal mode MLM output of an ion laser therefore has a coherence length of about 60 mm. A very narrow linewidth, which is required for OPC, is accomplished in an ion laser by installing an etalon in the laser cavity. This process will reject all the longitudinal modes except one and cause laser power to be concentrated in this single mode. Since a single longitudinal mode has a width of less than 3 Mhz the resulting coherence length can be more than 100 meters.
>
> The normal frequency spectrum of an ion laser is made up of 20 to 40 individual longitudinal modes covering a bandwidth of approximately 5 Ghz. Laser output using an etalon is known as Single Longitudinal Mode SLM or single frequency operation.

> An etalon when placed in the laser cavity acts as a bandpass transmission filter. The etalon will pass frequencies close to its transmission peak and reject, by reflection, frequencies outside the etalon passband.
>
> When an etalon passband moves to the point where it interacts with the next longitudinal mode. A mode hopping phenomena will occur. Mode hopping causes stepwise changes in the laser frequency which can result in frequency excursions of several thousand Mhz."

From this explanation, multi-mode laser energy causes some mode hoping within the OPC crystal. This causes a delay or even prevention of the phase conjugate process since the frequency is constantly shifting/hopping internal to the crystal. It is also recommended that the coherence length of the laser be measured to ensure that the wavefront is projected in phase along the entire path length of soot particle density path length L_e.

Thirdly, the use of retroreflectors and cubic quarter wave rotator beam spitters have the obvious effect of rotating the critical polarization of the laser beam. This will then result in the prevention of optical phase conjugation in a photorefractive crystal from occurring if the rotation is not accounted for in the initial setup.

Although OPC can be achieved with low power lasers, providing of course that the two above conditions are met, the system setup losses (by beam splitters, exhaust plume, etc.) requires that more power than that provided by a 10 mW Argon Ion laser be used. Principal system losses are contributed to the beam splitters which degrade the incident light energy below that which is required for the phase conjugate effect to occur. If a Faraday rotator, and a single mode laser were used, the 200-300 mW range may be sufficient.

In addition, a system which used a four-pass system vice the current two-pass system would allow for the Barium Titanate crystal to be collocated along with the entire laser apparatus. This would not only serve as a single unit setup but it would also provide equipment less susceptible to vibration. The depiction below (Fig. 5.2contains the necessary improvements. An alternative to the focusing lens in front of the phase conjugate crystal would be to use a top-hat beam sufficiently larger than the crystal. This would minimize beam steering effects which could cause the beam to not focus on the crystal. Although a barium titanate crystals can be grown to a 1 cm cube, their cost is prohibitive. Recent developments

in organic photorefractive crystals may reduce the cost and could also be grown to larger crystalline dimensions.

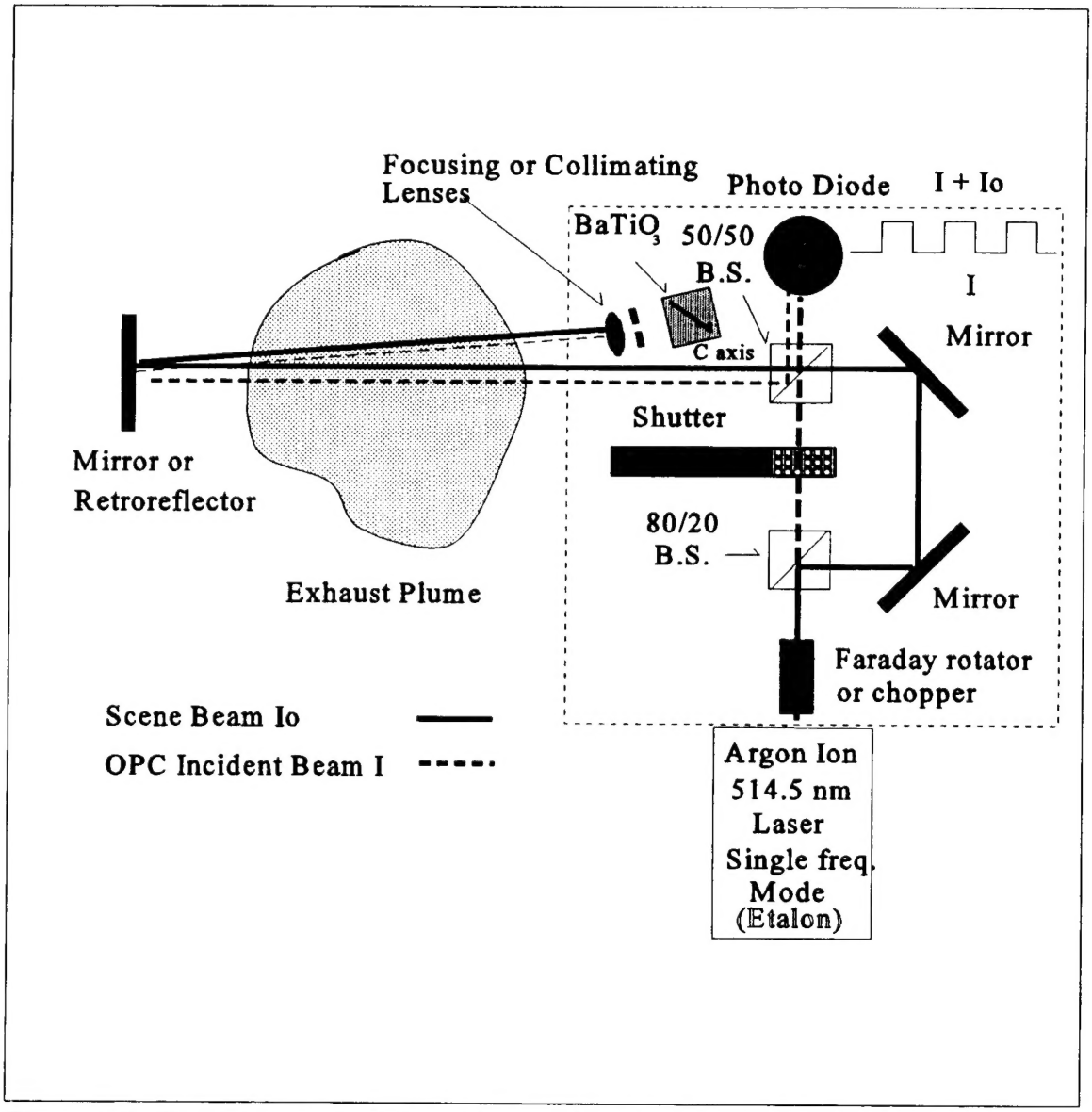

Figure 5.2. Four-Pass Optical Phase Conjugation with Argon Ion laser (Operating with a intercavity etalon providing a single frequency mode).

LIST OF REFERENCES

1. Biblarz, O., and Netzer, D.W., *Evaluation of UTSI-CLA Program on Optical Measurements of Turbine Engine Exhaust Particulates,* Naval Postgraduate School Technical Report, NPS-AA-94-001CR, January, 1994.

2. Shenoy, A.S., "*the Attenuation of Radiant Energy in Hot Seeded Hydrogen,*" PhD Dissertation, Georgia Institute of Technology, School of Nuclear Engineering, 164 pages (May 1969).

3. Dehne, H.J., "*Design, Construction and Preliminary Test of an Automated Isokinetic Sampler for Evaluating Particulate Emmisions from Aircraft Gas Turbine Engines*", Acurex Corp. Report 79-32/EE (December 1979).

4. Gould, R.K., Olson, D., B. and Calcote, H.F., *"Correlation of Soot Formation in Turbojet Engines and in Laboratory Flames"*, AFSC Report ESL-TR-81-09 (Feb. 1981).

5. Few, J., Lewis, J., and Hornkohl, J., *"Optical Measurements of Turbine Engine Exhaust Particulates"*, Naval Air Propulsion Center Report, NAPC-PE-221C, July 1991.

6. Powell, E.A., Casanova, R.A., Bankston, C.P., and Zinn, B.T., AIAA Paper No. 76-67, presented at the 14th AIAA Aerospace Sciences Meeting, Washington, D.C. (January 1976). Zinn, B.T., Powell, E.A., Casanova, R.A., and Bankston, C.P., Fire Research 1, 23 (1977). Chippett, S. and Gray, W.A., Combust. Flame 31, 149 (1978).

7. Cashdollar, K.L., Lee, C.K., and Singer, J.M., *"Three-wavelength Light ransmission Technique to Measure Smoke Particle Size andConcentration"*,Applied Optics, 18, pp. 1763 (1 June 1979).

8. Van de Hulst, H.C., *Light Scattering by Small Particles,* Dover Publication Inc., New York (1981), Chps. 1 and 9.

9. Kattawar, G.W. and Plass, G.N., *"Electromagnetic Scattering from Absorbing Spheres"*, Applied Optics, 6, pp 1377 (Aug. 1967).

10. Dobbins, R.A., Santoro, R.J., and Semerjian, H.G., *"Interpretation of Optical Measurements of Soot Flames"*, Combustion Diagnostics by Nonintrusive Methods, McCay and Roux Eds., AIAA Progress In Astronautics, 92 (1984).

11. Dobbins, R.A. and Jizmagian, G.S., J. Optics Society America 56, 1345 (1966).

12. Fisher, R.A., *Optical Phase Conjugation,* Academic Press, Inc., 1983.

13. Pepper, D.M., *Nonlinear Optical Phase Conjugation,* Elsevier Science Publishers, 1985.

14. Gunter, P., *Electro-Optic and Photorefractive Materials II,* Spring-Verlag Publishers, 1987.

15. Feinberg, J., *"Self-Pumped Continuous Wave Phase Conjugator Using Internal Reflection"*, Optics Letters, v.7, pp. 486-489, 1982.

16. Yeh, P., *"Photorefractive Phase Conjugators"*, Proceedings of the IEEE, v.80, pp. 436-450, 1992.

17. Ford, J.E., Fainman, Y., and Lee, H.L., *"Enhanced Photorefractive Performance from 45° - cut $BaTiO_3$"*, Applied Optics, v. 28, No. 22, (Nov. 1989).

18. Pepper, D.M., *"Hybrid Phase Conjugator/Modulators Using Self-Pumped O° -cut and 45° -cut $BaTiO_3$ Crystals,"* Applied Physics Letter 49, 1001-1003 (1986).

19. Brody, P.S. and Goff, J.R., *"Grating Evolution and Form in a Single-Crystal Self-Pumped Barium Titanate Phase Conjugator,"* Proceedings of SPIE, v.739, Phase Conjugation and Beam Combining and Diagnostics, pp. 50-56, (Jan 1987).

20. Zhank, G., Li, Q., Ho, P., Liu, S., Wu, Z.K., and Afano, R.R, "Dependence of specklon size on laser Beam Size via Photo-Induced Light Scattering in $LiNbO_3$:Fe," Applied Optics 25, pp. 2955-2959.

INITIAL DISTRIBUTION LIST

		No. Copies
1.	Defense Technical Information Center Cameron Station Alexandria, Virginia 22304-6145	2
2.	Library, Code 52 Naval Postgraduate School Monterey, California 93943-5101	2
3.	Prof. O. Biblarz, Code AA/Bi Naval Postgraduate School Monterey, California 93943-5106	3
4.	Prof. D.W. Netzer, Code AA/Nt Naval Postgraduate School Monterey, California 93943-5106	2
5.	Chairman Space Systems Academic Group, Code SP Naval Postgraduate School Monterey, California 93943-5101	1
6.	Chairman Dept. of Aeronautics and Astronautics, Code AA Naval Postgraduate School Monterey, California 93943-5101	1
7.	Mr. William Voorhees Code PE34 Naval Air Warfare Center, Aircraft Division Trenton, New Jersey 08628-0176	4
8.	LT Gregory E. Glaros 312 Spice Bush Court Chesapeake, Virginia 23320	4